Crack propagation and deviation in bi-materials under thermo-mechanical loading

Mourad Chama[*1], Benali Boutabout[1], Abdelkader Lousdad[2], Wafa Bensmain[1]
and Bel Abbes Bachir Bouiadjra[1]

[1]*Laboratory of Mechanical and Physical of Materials (LMPM), University Djillali Liabes of Sidi Bel Abbes, BP 89, Street Ben M'Hidi, Sidi Bel Abbes, Algeria*
[2]*Laboratory of Mechanics of Structures and Solids (LMSS), University Djillali Liabes of Sidi Bel Abbes, BP 89, Street Ben M'Hidi, Sidi Bel Abbes, Algeria*

Abstract. This paper presents a finite element based numerical model to solve two dimensional bi-material problems. A bi-material beam consisting of two phase materials ceramic and metal is modelled by finite element method. The beam is subjected simultaneously to mechanical and thermal loadings. The main objective of this study is the analysis of crack deviation located in the brittle material near the interface. The effect of temperature gradient, the residual stresses and applied loads on crack initiation, propagation and deviation are examined and highlighted.

Keywords: elasto-plastic; finite elements method (FEM); fracture mechanics; interface problems; numerical methods; crack/ damage detection/identification

1. Introduction

During these last years, the research carried out led to the development of the ceramics with high performance which makes them occupy an increasingly significant place in the industry sector. Ceramics such as zircon, carbide silicon, silicon nitrides and alumina have a great number of applications in the mechanical and thermal field. If the three first are still of limited use, this is not the case for the alumina which remains the most widely used technical ceramics. Besides the mechanical applications, it takes the first place in the electronics industry because of its good dielectric property. To benefit from the maximum of these properties, these materials are often used jointly with metals or metal alloys to make bi-materials or multi-materials. The extension of their use requires thorough studies.

Joining ceramics to metal is inherently difficult because of their distinctly different properties and because of the damage occurring in the weakest zone of the bi-materials. However considerable efforts devoted to the development of joining technologies in recent years have led to significant success (Boutabout *et al*. 2009, Boutabout *et al*. 2004, Serier *et al*. 1993). The case of crack along the interface between brittle and ductile materials has been investigated extensively,

---

*Corresponding author, Ph.D. Student, E-mail: chamagm10@yahoo.fr

both experimentally (Mc Naney *et al*. 1994) and theoretically (Shih and Asaro 1988, Tvergaard and Hutchinson 1993). The case of the crack oriented parallel to the interface at a small distance away from it received less attention (Cao *et al*. 1998, Fleck *et al*. 1991). Experimental tests showed that the breaking strength of the interface and ceramics in the vicinity of the interface depends on the difference between the mechanical and physical properties of both bonded materials (Liu 2005, Siddiq 2006, Shanahan 1991). The cohesive fractures in alumina are observed on levels of stresses much lower than the fracture strength of the same material alone not assembled with a metal (Mc Bain and Hopkins 1925, Juvé *et al*. 1993). Engineering structures and components subjected to the combination of residual stresses with operating stresses on can promote failure by fatigue. The effect of residual stresses on the crack propagation was studied by several authors (Itoh *et al*. 1989, Kang *et al*. 1990, Barsoum 2008). This influence is considered as one of the most significant factors to predict the crack growth rates. The combined effect of residual stresses and applied load may cause an assembly to fail sooner than expected and reduced durability due to damage mechanisms. Kim *et al*. (2012) measuring high speed Crack propagation in concrete fracture test using mechanoluminescent material. Kumar and Barai (2012) analysed Size-effect of fracture parameters for Crack propagation in concrete. Jiang *et al.* (2014) presented An investigation into the effects of voids, inclusions and minor Cracks on major Crack propagation by using XFEM.

The tensile residual stresses decrease the fatigue life of the structure while compressive ones increase the fracture resistance, contribute to crack closure and reduce the crack opening profile (Milan and Bowen 2000, 2001). The fracture behaviour of bi-materials is studied by numerical simulation using finite element method. Our Analysis highlights the influence of a thermo-mechanical loading on crack propagation and deviation.

2. Geometrical model

The geometrical model is a beam which consists of two materials ceramic-metal of dimensions (55mm×6mm×6mm). The beam is submitted to four-points bending (4PB) test. The bi-materials joints typically contain residual stresses (Lourdin 1992, Courbiere 1986, Belhouari 2004, Bouchard 2000, Shandhag *et al*. 1993, Simmons and Wang 1971, Touloukian 1967, Follansbee and Gray 1991, Crandall *et al*. 1978, Chawla 1987) that arise during the fabrication process when the joints are cooled from high temperature T_{el} (near the melting point of metal) to the ambient temperature T_{am}. The temperature distribution in the assembly was assumed to be homogenous. The initial edge crack length is a_0. The beginning in the vicinity of the interface ceramic-metal (x=0.1mm) and is oriented parallel to this interface Fig. 1(a) (Kim and Lee 1998).

In this numerical analysis of the finite element method, the specimen models in two dimensions under plane stress conditions. It is meshed by quadrilateral elements with eight nodes as shown in Fig. 1(b). The mesh contains 93598 nodes and 30749 isoparametric elements. In order to obtain accurate stresses the mesh is relatively refined at both interface and crack-tip zones respectively as shown in Fig. 1(c).

3. Thermo-mechanical properties of materials

Mechanical tests (4PB) showed that the breaking strength of the interface and ceramics in the
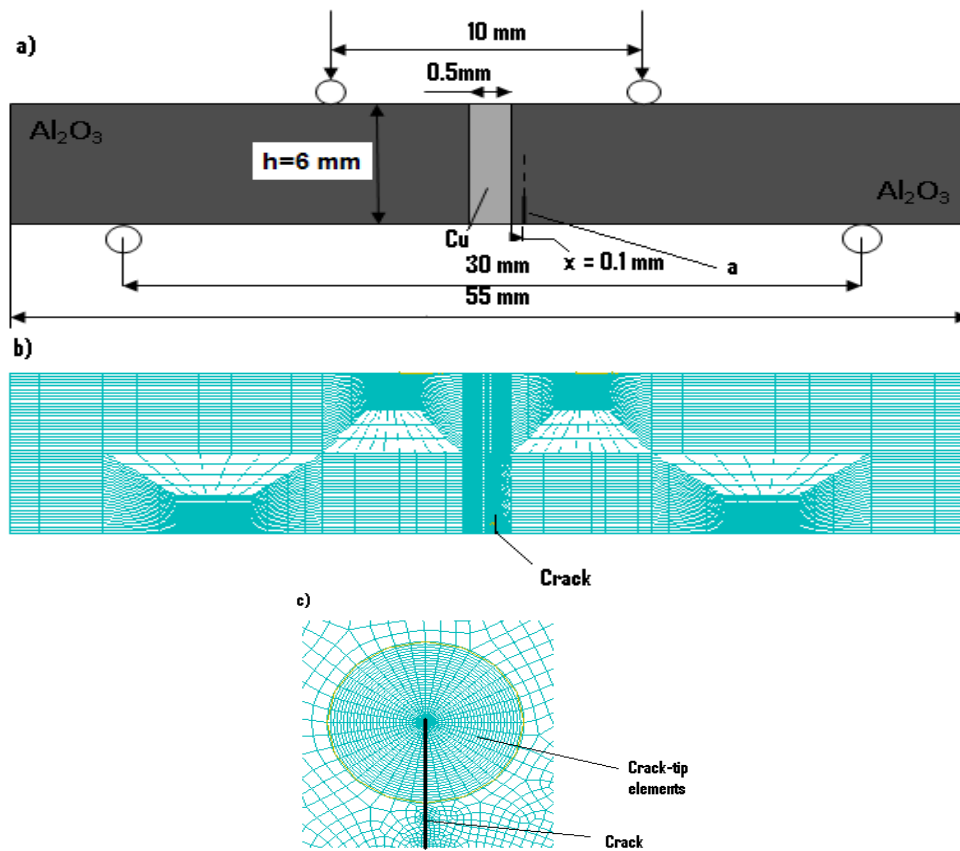
Fig. 1 (a) Geometrical model, (b) Representative finite-element mesh of assembly and (c) mesh near the crack-tip

Table 1 Thermo-mechanical properties of alumina (Al$_2$O$_3$)

E [GPa]	μ [GPa]	v	α [10^{-6} /°C]	λ [wm^{-1} K^{-1}]	K_{IC} [MPa m$^{-1/2}$]
385.8	155	0.245	7.12	35	3.5 a 4.5

Table 2 Thermo-mechanical properties of copper (Cu)

E [GPa]	μ [GPa]	v	α [10^{-6} /°C]	λ [wm^{-1} K^{-1}]
124	42.20	0.328	17.5	385

vicinity of the junction depends on the difference between the mechanical properties of the two assembled materials (Courbiere 1986, Belhouari 2004, Bouchard 2000). Generally, the melting point and a mechanical resistance of the alumina have been higher than those of copper. Consequently, a ductile material has elastic-plastic behaviour and that of a brittle material is purely elastic. The mechanical and physical properties of both materials alumina and copper can be found in reference (Boutabout *et al*. 2009, Aide-mémoire de science des matériaux 2004) and are summarized in Tables 1-2.
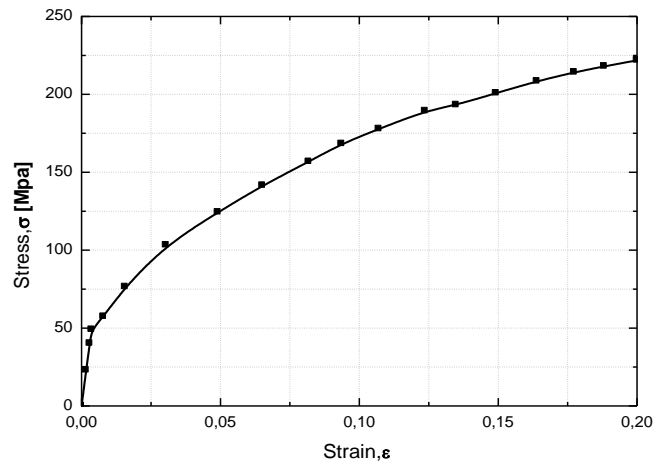
Fig. 2 Non-linear deformation behaviour for a copper, taken from experimental results (Chapa-Cabrera and Reimanis 2002)

3.1 Thermo-mechanical properties of alumina

Alumina is the first basic compound for technical ceramics because of its exceptional versatility: abrasion, wear, refractory, biomedical…etc. Alumina is classified in the category of oxide ceramic type. It defines the corundum structure where the oxygen form has a hexagonal compact stacking with the aluminium ions in the two thirds of octahedral pattern. This lowers the structure of alumina has two types of sites, hexagonal and octahedral in which it holds the atoms. Alumina is used because of its strong atomic bonds, its high mechanical and thermal performance (high hardness, high modulus of elasticity, satisfactory mechanical resistance, wear resistance as well as its properties of stability, purity and refractoriness) and it is expressed by the formula Al_2O_3 (Simmons and Wang 1971).

3.2 Thermo-mechanical properties of copper

The physical and mechanical properties of copper are available in the literature (Follansbee and Gray 1991, Crandall *et al*. 1978). This ductile material with a crystalline structure (face centred cubic), is a good conductor of heat and electricity. It has solid solutions at high temperature and a good tensile strength. Generally, it can have several behaviours (elastic, elastic-plastic, plastic…). In this investigation, the behaviour of copper is assumed to obey stress-strain law as shown in Fig. 2 (Chapa-Cabrera and Reimanis 2002) and is assumed symmetrical in tensile and compression.

4. Finite element method

Our analysis focuses on the effect of thermo-mechanical loading on crack propagation and its deviation using finite element method with the software Abaqus (ABAQUS Standard Version 6.9. 2009). The choice of mesh elements may be crucial because an inappropriate mesh can lead to erroneous results (Bouchard 2000). In order to obtain satisfactory results, it is necessary to know

how to mesh the structure. One should know that a refined mesh gives a good accuracy. The approach adopted in this analysis is to use a reasonable mesh while refining mesh of critical areas such as the interface, the crack tip and four-point bending. A good mesh is obtained by ideal refining very close to the interface and the crack-tip. It is made of an optimal number of elements that is able to provide accurate results with a reasonable mesh. We determined numerically by the finite element method the opening and sliding of the crack (u_1, u_2) and *J*-integral, in plane stress conditions, these results are used to determine respectively, the SIF's K_I, K_{II}, K_{DCT} and the SIF K_J.

4.1 Computation of the stress intensity factor in mode I and II

Mode I and Mode II stress intensity factors, K_I and K_{II}, are calculated by correlation of nodal displacements near the crack-tip

$$\mathrm{K}_\alpha = \lim_{r\to 0}\left[\frac{u_i E_{tip}}{(2+2\upsilon_{tip})g_i^{(\alpha)}(\pi)}\sqrt{\frac{\pi}{8r}}\right] \qquad \{\alpha, i\} = \{\mathrm{I}, 2\}, \{\mathrm{II}, 1\}, \{\mathrm{III}, 3\} \qquad (1)$$

Where:

K_α (α=I,II) are the stress intensity factor in the mode I and II, *r* is the distance of the correlation point from the crack-tip, E_{tip} and ν_{tip} are Young's modulus and Poisson's ratio at the crack-tip.

$g_i^{(\alpha)}(\theta)$ are angular functions given by Anderson (Anderson 1995).

From these, the total stress intensity factors obtained using the displacement correlation technique (DCT), K_{DCT}, is calculated as

$$\mathrm{K}_{DCT} = \sqrt{\left(\mathrm{K}_I^2 + \mathrm{K}_{II}^2\right)} \qquad (2)$$

J-integrals are also calculated, by integration along a path outside the region of plastic yielding which exists in ductile materials. Values of K_J obtained from *J*-integrals, enabled the verification of stress intensity factor values

$$(3)$$

$$\mathrm{K}_J = \sqrt{(J \bullet E)}$$

The crack propagation in mixed mode and its deviation in the ceramics depend on the thermal stress and that bending field which vary proportionally with the applied load P_n for ($n = 1, 2….$). The stress intensity factor of equivalent stress reaches the tenacity of a brittle material for the critical load P_n.

4.2 Determination of the crack deflection angle

The mixed mode, ψ, was calculated from stress intensity factor in mode I and II determined by crack opening and sliding displacements (COD, CSD) (Chapa-Cabrera and Reimanis 2002)

$$\psi = \tan^{-1}\left(\frac{\mathrm{K}_{II}}{\mathrm{K}_I}\right) \qquad (4)$$

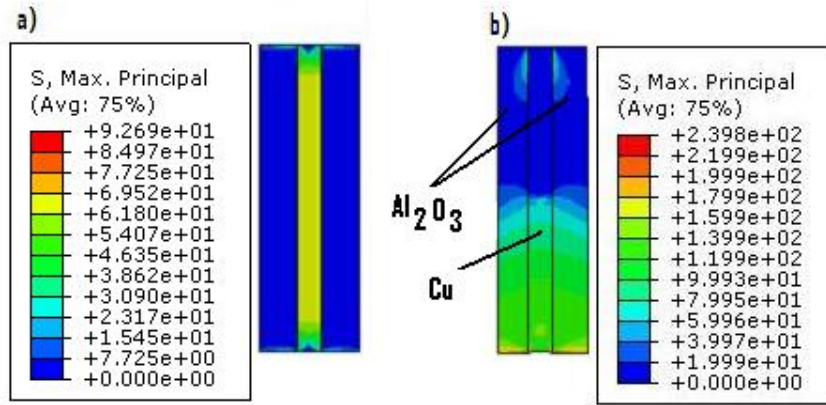For the maximum tangential stress (MTS) criterion, the deflection angle, θ, is calculated directly from ψ

Fig. 3 Contour of the equivalent stress in Al$_2$O$_3$/Cu/Al$_2$O$_3$ a) residual and b) Specimen under four point bend loading

$$\tan\left(\frac{\theta}{2}\right) = \frac{2 - 2\sqrt{1 + 8\tan^2\psi}}{8\tan\psi} \tag{5}$$

Traditionally, these deflection criteria have been developed for predicting the crack propagation direction in brittle materials, under stress conditions for small crack size.

5. Results and discussions

5.1 The distribution of the stress in the couple Al$_2$O$_3$/Cu/Al$_2$O$_3$

Figs. 3(a)-(b) show respectively the distribution, the level of the equivalent residual stress and that mechanical stress developed in the bi-materials alumina-copper-alumina without the presence of a crack in the ceramic. Fig. 3(a) illustrates the contour of the equivalent thermal stress in the assembly at the free edge near the interface which reaches a maximum value calculated according to the criterion of the maximum principal stress. Numerical analysis of the four points bending (4PB) test has allowed determining the stress contour as displayed in the Fig. 3(b). It is observed that the upper part of the beam is subjected to compressive stresses whose absolute value is less than those of traction created at the lower part of the specimen. The variation of the equivalent stress at a distance from the interface-ceramics for thermal and mechanical loading applied separately on the bi-materials are shown in Fig. 4. One can note that the curve of the residual and bending stresses are almost similar. The equivalent stress reaches a maximum value in the vicinity of the interface and it decreases gradually as it moves away from the junction of the assembly. It is observed that bending stress is more intense than those caused by the thermal loading.

5.2 Determination of the stress intensity factor

5.2.1 Effect of temperature and crack size on the parameter K_J
The variation of the equivalent stress intensity factor (SIF) K_J (calculated by the *J*-integral) as a
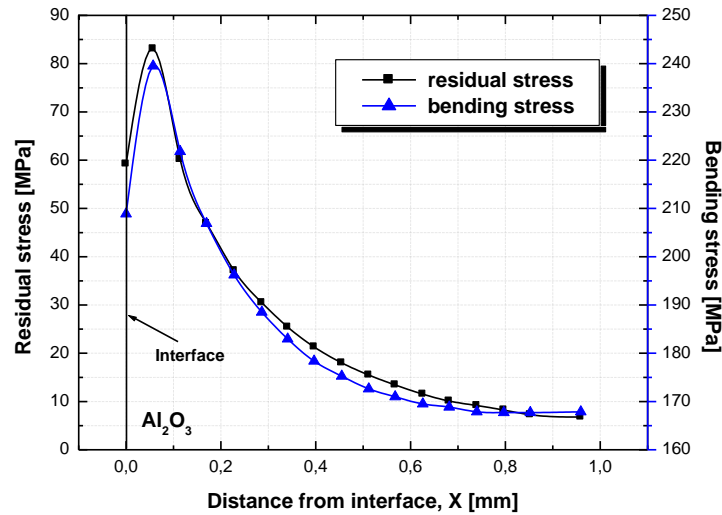
Fig. 4 Variation the residual stress and four points bending stress distribution in alumina of the assembly ($Al_2O_3/Cu/Al_2O_3$)
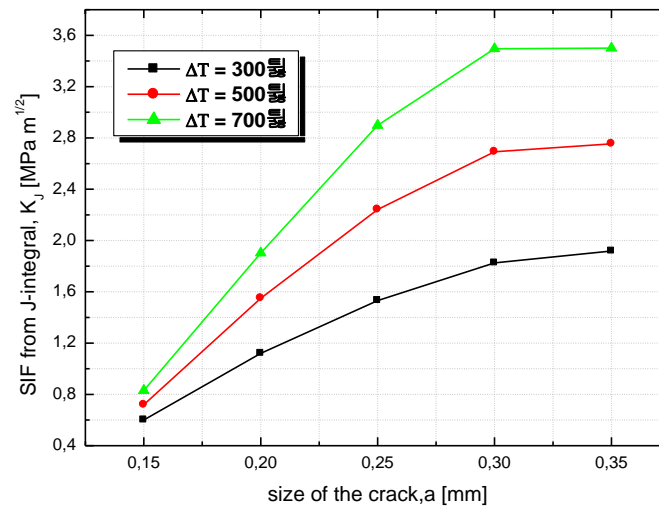

Fig. 5 Variation the stress intensity factor K_J obtained from *J*-integral as a function of crack size and temperature gradient ΔT

function of the crack size at three temperature gradient 300℃, 500℃ and 700℃, is displayed in Fig. 5. It can be seen that the parameter K_J vary almost linearly with the crack size and whatever the elaboration temperature T_{el} of the bi-materials is (near the melting point of metal). It should be noted, that for small crack lengths the parameter K_J tends towards an asymptotic value meaning that the crack propagation of shorter lengths is independent of the thermal residual stress. It is also noticed that the variation of the equivalent stress intensity factor K_J increases with the increase in temperature gradient ΔT and the crack size. It is observed that the change of the parameter *K* is 82% of crack length equal to 0.35mm and between the extreme temperatures. Stress intensity
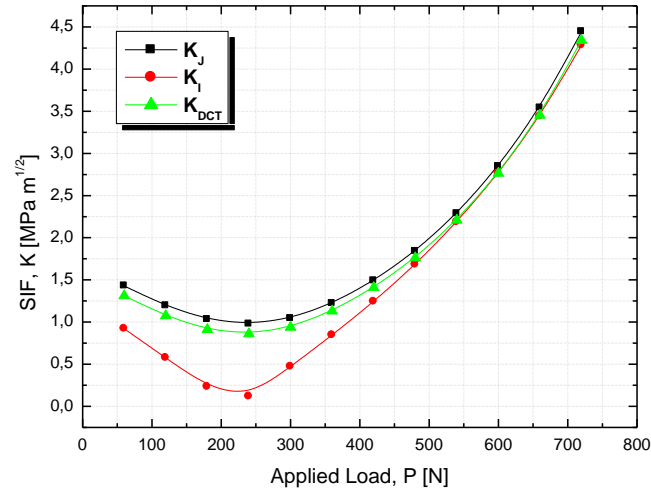
Fig. 6 Comparison of stress intensity factors (K_I, K_{DCT}) obtained using the displacement correlation technique (DCT) and those obtained from *J*-integral for a crack length 0.35 mm with $\Delta T = 300\,°C$

factor reaches its breaking value when the bi-materials are assembled at a temperature close to the melting point of copper and presenting a big size of crack located in alumina.

5.2.2 The effect of thermo-mechanical loading on the SIF

The relationship between actual stress intensity values, as calculated from the *J*-Integral, and apparent SIF values, as calculated from crack-opening displacements, is illustrated in Fig. 6. The results are determined for a crack length 0.35 mm with $\Delta T = 300\,°C$. These results obtained numerically by the finite element method show that whatever the value of the applied load *P* is the shape of the two curves K_J and K_{DCT} is almost similar. This shows that there is a clear empirical relationship, so stress intensity factors may be calculated from crack-opening displacement. We note that the values of the parameters K_J and K_{DCT} show a good agreement in this case (elastic behaviour). It is noted that, the three parameters K_I, K_{DCT} and K_J increase quickly beyond the applied load $P=400$ N with at high increasing rate.

The curve takes the parabolic form for which the three parameters decrease with increasing the mechanical stress down to a minimum value then increase gradually up to a maximum value.

The minimal values of the stress intensity factor K_J and K_{DCT} correspond to the propagation of the crack in pure mode II. Results found previously are validated by those of the stress intensity factor in mode I (K_I) as shown in Fig. 6. Beyond the applied load $P=600$ N, the three curves show that crack propagates in pure mode I.

Fig. 7 shows the variation of the parameter K_J as a function of thermo-mechanical loading for a crack length $a=0.35$ mm. The parameter K_J increases proportionally with the temperature gradient for longer crack lengths. It is also observed that the parameter K_J decreases gradually with increasing the applied load to reach a minimum value which depends on the thermal loading and then rises again to reach a maximum value. The lowest values of K_J are proportional to the elaboration temperature and the applied load for which the propagation of the crack is in pure mode II. Beyond this minimum value of the SIF K_J the crack continues to propagate in mixed mode under the effect of thermo-mechanical loading with increasing applied load. For important
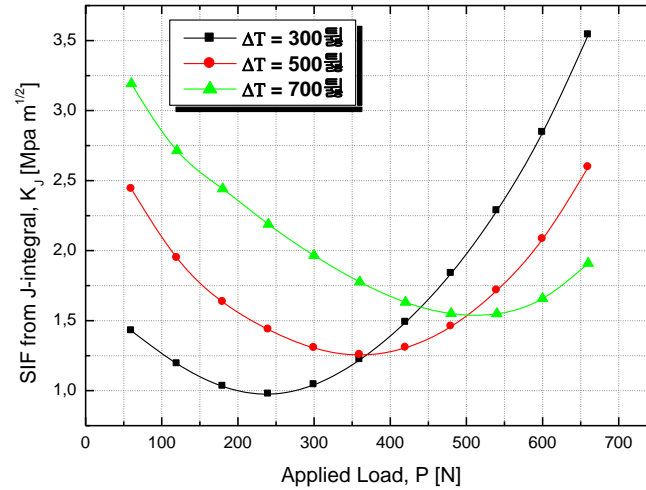
Fig. 7 Variation the stress intensity factor K_J obtained from J-integral as a function of thermo-mechanical loading with the crack length a=0.35 mm
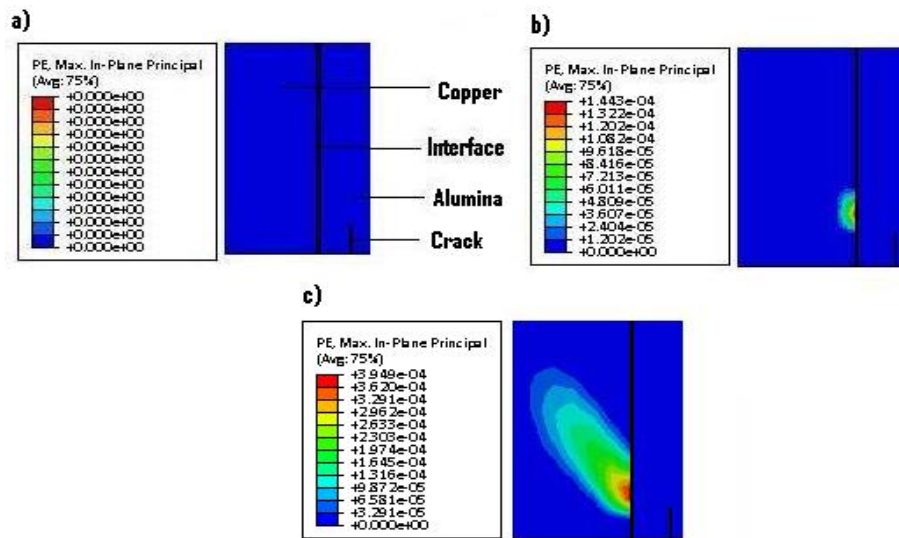

Fig. 8 Plastic strain fields in the copper near a crack situated 0.35 mm from the interface, for applying loads (a) 300N, (b) 360N and (c) 420N

loads the crack is propagated in mode I and II only under the effect of the bending stress field and the influence of thermal loading which tends to disappear. The tensile stresses overcome the compressive thermal residual stresses. The bending of the beam leads to the propagation of the crack in mixed mode, however the normal residual stresses cause the closing of the crack and those of shearing lead to sliding of the cracked lips in the direction opposite to that of bending tangential stresses.

Fig. 8 presents the contour of the plastic strain fields. It should be noted that the plastic zone appears in the ductile material and more precisely in the vicinity of the crack-tip. The growth of
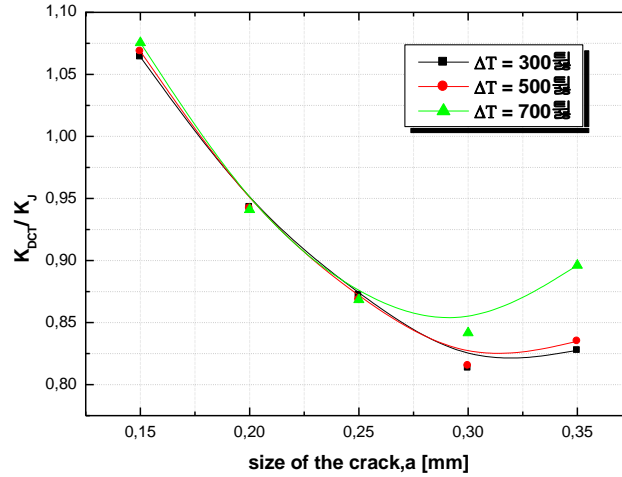
Fig. 9 Variation the ratio K_{DCT}/K_J as a function of crack size and temperature gradient ΔT

the plastic zone increases with increasing applied load. Plastic strain is accompanied by energy absorption which promotes stress relaxation at the crack-tip. This phenomenon slows down the crack propagation and it probably influences the crack deviation. The minimum value of stress intensity factor K_J is mainly due to the appearance of the plastic zone in ductile materials.

5.2.3 The variation of the K_{DCT}/K_J

Fig. 9 shows the variation of the ratio K_{DCT}/K_J as a function of temperature gradient and for various crack lengths. This figure shows that the two stress intensity factors K_{DCT} (calculated by K_I and K_{II}) and K_J are equal for a crack equal to 0.175 mm. It is also observed that both curves determined respectively for the two temperature gradient 300℃, 500℃ are coincident. The ratio K_{DCT}/K_J decreases gradually with increasing crack size from 0.15mm to 0.35mm. We note that the maximum difference between the two stress intensity factors K_{DCT} and K_J is about 27%. The third curve corresponding to ΔT=700℃ is coincident with the two previous plots up to a crack length equal to a crack length equal to 0.25 mm. Beyond this value we note that the ratio increases again with the crack size.

5.2.4 Effect of thermo-mechanical loading on crack propagation in mixed mode

Fig. 10 illustrates the variation of the ratio K_I/K_{DCT} as a function of thermo-mechanical loading with the crack length a=0.35 mm. According to this figure, we notice that the shape of the curve is the same for the three elaboration temperatures. It is noticed that for the low mechanical loads, the crack is propagated in mode I which is dominated by the compressive residual stresses causing the crack closure. The ratio K_I/K_{DCT} vanishes for three temperature gradients which correspond to minimum values of the SIF K_J (Fig. 7). Indeed, the increase in the applied load leads to the opening of the crack in mode I.

The variation of the ratio K_{II}/K_{DCT} as a function of thermo-mechanical loading when the crack length equal to 0.35 mm, is represented in Fig. 11. It is noticed that whatever the temperature gradient the three curves of the ratio K_{II}/K_{DCT} are identical. The maximum absolute values of the ratio K_{II}/K_{DCT} correspond to the crack propagation in pure mode II. These results show clearly that the intensity of residual shear stresses increases with the temperature and is more significant than
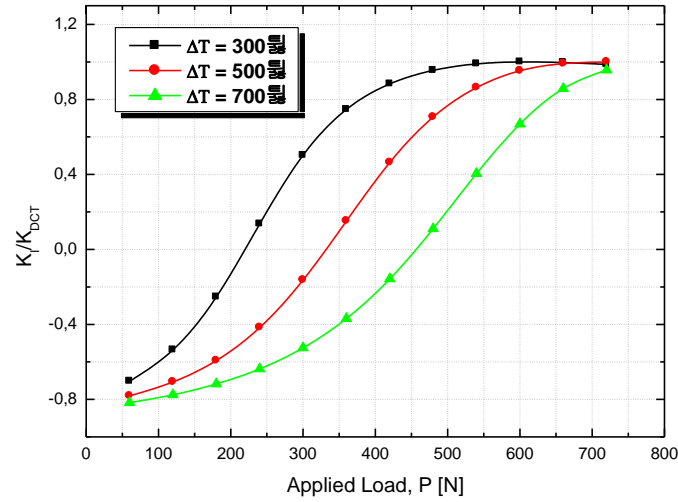
Fig. 10 Variation the ratio K_I/K_{DCT} as a function of thermo-mechanical loading with the crack length a=0.35 mm
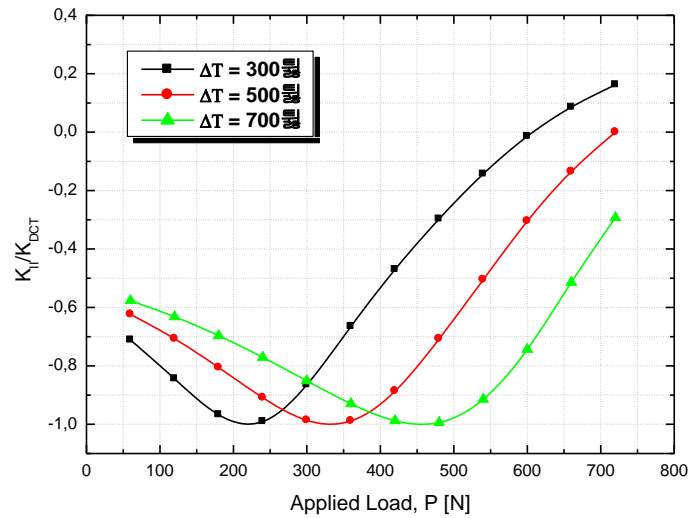

Fig. 11 Variation the ratio K_{II}/K_{DCT} as a function of thermo-mechanical loading with the crack length a=0.35 mm

that of the bend for low mechanical loading. The effect of the latter on the propagation in mode II appears in higher applied loads to the beam and small temperature gradients.

However, it is noted that this effect tends to disappear when the applied load increases. It is observed that the ratio K_{II}/K_{DCT} reached the maximum value for the three temperature gradients 300°C, 500°C and 700°C respectively for the corresponding loads of 215 N, 335 N and 450 N. It is noted that the maximum value of the ratio K_{II}/K_{DCT} corresponds to the applied load whose intensity depends on the elaboration temperature. Indeed, the level of the thermal stresses is important for high temperature, which requires higher bending to overcome the thermal stress.
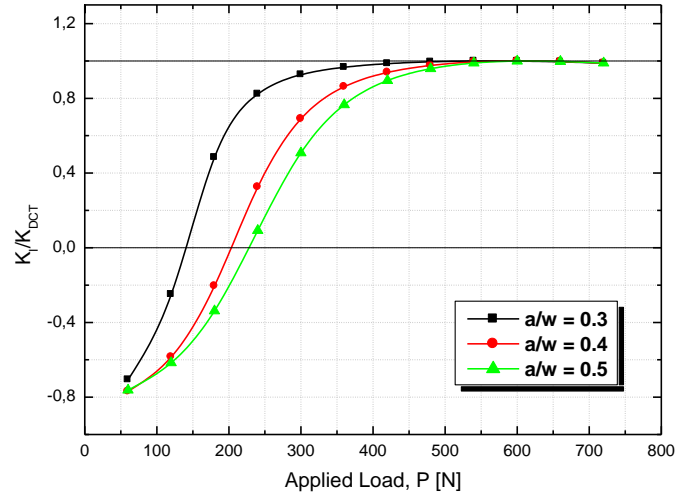
Fig. 12 Variation the ratio K_I/K_{DCT} as a function of applied load P and ratio a/w (w=0.5 mm) with the temperature gradient ΔT=300°C
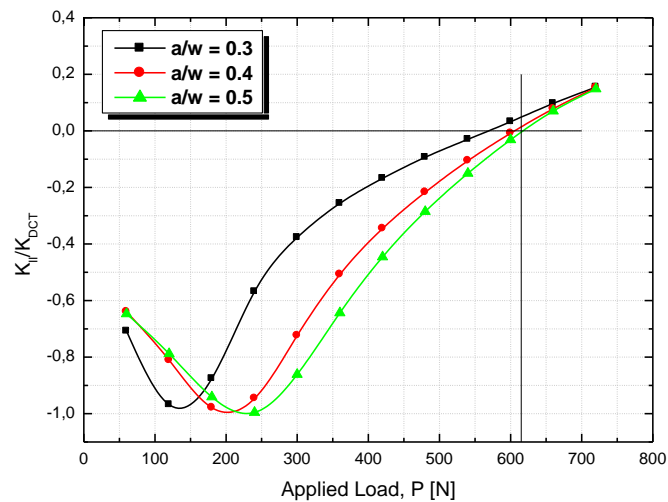

Fig. 13 Variation the ratio K_{II}/K_{DCT} as a function of applied load P and ratio a/w (w=0.5 mm) with a temperature gradient ΔT=300°C

5.2.5 Effect of thermo-mechanical loading and crack size on crack propagation in mixed mode

The variation of the ratio K_I/K_{DCT} as a function of applied load P and crack length with the temperature gradient equal to 300°C is represented in Fig. 12. The results show that the shapes of the three curves are similar and the pilot's approach each other gradually as the crack size increases. It is noticed that for the three crack sizes, the ratio K_I/K_{DCT} tends towards two asymptotic values -0.80 and 1.00 respectively for the lowest and the highest loads. It is noted that for the ratio a/w=0.3 (w=0.5 mm) and for loads less than 140 N, the thermal stress field causes the closing of the crack. By exceeding this load, the bending stress field leads to the propagation of the crack in

mixed mode. The SIF K_I vanishes for P=140 N for which the crack is propagated in pure mode II. Indeed, the same behaviour in rupture is observed for the two ratios a/w=0.4 and a/w=0.5. The ratio K_I/K_{DCT} is zero for loads 200 N and 225 N which correspond to the two crack lengths a=0.4 w and a=0.5 w respectively.

The variation of the ratio *KII/KDCT* as a function of applied load P and crack length when the temperature gradient equal 300℃, is represented in Fig. 13. It is noticed that the two curves determined for the two crack lengths a=0.4 w and a=0.5 w are almost identical. We note that the crack is propagated in pure mode II for the ratios a/w=0.3, a/w=0.4 and a/w=0.5 and the respective loads of 140 N, 200 N and 225 N for which the ratio *KII/KDCT* reached a maximum absolute value equal to unity. This confirms the results found previously as shown in Fig. 12. It is also noticed that the crack is propagated in pure mode I when the residual shear stresses are balanced with those of the bending stress. The effect of the thermal loading disappears for the crack lengths a=0.3 w, a=0.4 w and a=0.5 w with the respective loads of 575 N, 600 N and 610 N and the crack is propagated in mixed mode under the effect of the bend.

5.3 Deviation of the crack

5.3.1 Effect of thermal loading and crack size on the deflection angle θ
Fig. 14 illustrates the variation of the deflection angle θ as a function of thermal loading and crack size.

It is noted that under thermal loading the crack is propagated towards brittle material and the deflection angle θ increases with the crack size. It is observed that this deflection angle is inversely proportional to the temperature gradient. The normal residual stresses are involved in the closure of the crack and prevent its deviation towards the ceramic.

5.3.2 Effect of thermo-mechanical loading and crack size of the deviation
Fig. 15 presents variation of the deflection angle θ as a function of thermo-mechanical loading. The crack length a=0.35 mm is initially in the brittle material (Al_2O_3) the vicinity of the interface;
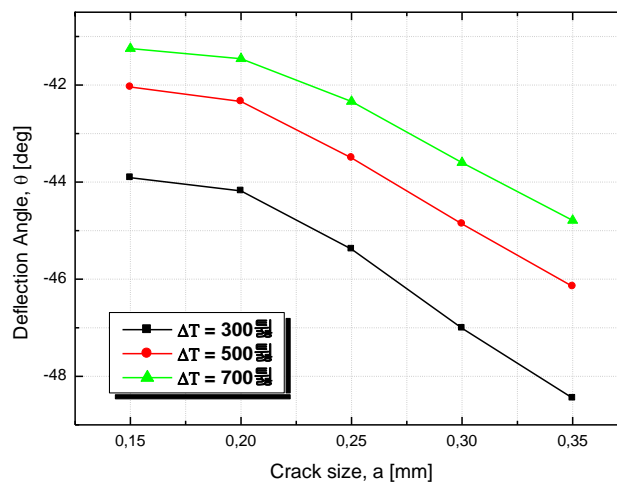
Fig. 14 Variation the deflection angle θ as a function of thermal load and crack size
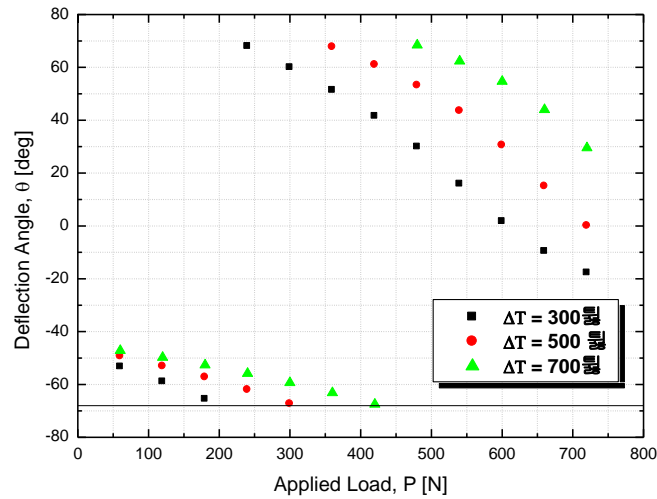
Fig. 15 Variation the deflection angle θ as a function of thermo-mechanical load with the crack length equal 0.35 mm

it is subjected to thermal and mechanical loads. Whatever the elaboration temperature is, we observe that the deviation of the crack in the brittle material increases almost linearly with the applied load. Indeed, the crack is deviated towards the ceramic from the angle θ equals to approximately -50° to 68°. The first angle is obtained for the lowest load and the second angle θ corresponds to the three temperature gradients 300°C, 500°C and 700°C with respective loads 180 N, 300 N and 420N. We note that for the three temperature gradients ΔT a discontinuity of the deflection curve for the respective loads of 215 N, 235 N and 450 N for which the angle is zero and therefore the crack is propagated in pure mode II (Fig. 11). When the residual shear stresses are relatively more significant than those of the bending and the normal residual stresses are balanced with those of the bending stress then the crack changes suddenly its deviation towards the ductile material. The deviation to the metal is recognized when the bending stress exceeds a critical value of 240 N, 360 N and 470 N respectively correspond to the elaboration temperature of 300°C, 500°C and 700°C. It is also noticed that this deflection decreases with increasing bending stresses. It is observed that the SIF K_I increases with increasing applied load whereas the SIF K_{II} is inversely proportional to the load P.

The variation of the deflection angle as a function of load P and crack size with the temperature gradient ΔT=300°C is represented in Fig. 16. According to this figure, we observed that for a low thermal loading, the shape of the deviation curve is almost the same for the three crack lengths. The deflection angle tends towards an asymptotic value in the ceramic and metal, respectively for low and high loads P. We also note that the angle increases slightly with the crack size when it begins to change its direction towards the ductile material. For the weak mechanical loads the crack-tip is under the compressive stress field higher than the tensile stress field and the crack is propagated in mixed mode. The crack propagation in mode I relatively lower than mode II and consequently it moves towards the brittle material and its deflection angle θ increases with the applied load. Once the crack is propagated in pure mode II (Fig. 13), it changes direction and moves towards ductile material of which the angle θ gradually decreases with increasing load. It vanishes when the crack propagation is in pure mode I (Fig. 12) for higher applied loads and the
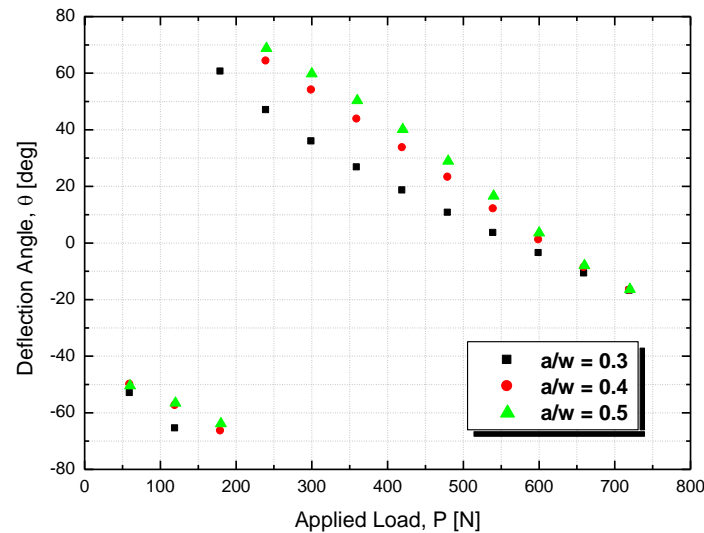
Fig. 16 Variation the deflection angle θ as a function of applied load P and crack size with the temperature gradient $\Delta T = 300°C$

contribution of mechanical loading on the crack propagation in mixed mode becomes more significant.

It can be concluded that for low loads the crack propagation in mixed mode is mainly due to the dominant effect of thermal loading. However, the increase in load creates the high tensile stress field where propagation crack is still in mixed mode while at this time the effect of the compressive stress field becomes less important. Indeed, the external load exceeds a critical load which can cause a great risk of damage of the bi-materials Cu/Al_2O_3 and can lead to a fast propagation of the crack which will be deviating towards the ductile material (Cu).

6. Conclusions

The analysis of fracture behaviour of the bi-materials Cu/Al_2O_3 allows drawing the following conclusions:

- The equivalent SIF K_J depends on both loading of thermal and mechanical stress fields developed at the crack-tip;
- The Crack size has an effect on the variation of equivalent stress intensity factor K_J;
- The Plastic zone of ductile material has an effect on the crack propagation;
- We note that the values of the parameters K_J and K_{DCT} show a good agreement in this case (elastic behaviour);
- The crack propagation in mixed mode depends on the thermo-mechanical loading;
- The temperature gradient and the applied load have an effect on the crack deviation;
- The crack propagation in pure mode I or pure mode II corresponds to a deflection angle equals to zero.

References

Anderson, T.L. (1995), *Fracture mechanics: fundamentals & applications*, CRC Press, Boca Raton (FL).

Barsoum, Z. (2008), "Residual stress analysis and fatigue of multi-pass welded tubular structures", *Eng. Fail. Anal.*, **15**, 863-874.

Belhouari, M. (2004), "Etude du comportement en rupture des bi-matériaux", Thèse de Doctorat d'Etat, Université de Djillali Liabes, Sidi Bel Abbes.

Boutabout, B., Chama, M., Bouiadjra, B.A.B., Serier, B. and Lousdad, A. (2009), "Effect of thermomechanical loads on the propagation of crack near the interface brittle/ductile", *Comp. Mater. Sci.*, **46,** 906-911.

Boutabout, B., Serier, B., Bachir Bouiadjra, B. and Tréheux, D. (2004), "Junction Ni/Al$_2$O$_3$ elaborated by thermo-compression: Determination of the thermal residual stresses", *J. Mech. Adv. Mater. Struct.*, **11,** 93-107.

Bouchard, P.O. (2000), "Contribution à la modélisation numérique de la rupture et structures multi-matériaux", Thèse Doctorat, Ecole Nationale Supérieure des Mines, Paris.

Cao, H.C., Thouless, M.D. and Evans, A.G. (1998), "Residual stresses and cracking in brittle solids bonded with a thin ductile layer", *Act. Meter.*, **36**(8), 2037-2046.

Chapa-Cabrera, J.G. and Reimanis, I.E. (2002), "Effects of residual stress and geometry on crack kink angles in graded composites", *Eng. Fract. Mech.*, **69**, 1667-1678.

Chapa-Cabrera, J.G. and Reimanis I.E. (2002), "Crack propagation in CuW FGM", *Philos Mag. A*, **82**(17-18) 3393-3403.

Chawla, K.K. (1987), *Composite Materials: Science and Engineering*, Springer, Berlin.

Courbiere, M. (1986), "Etude des liaisons céramique-métal, application au couple Cu/Al2O3", Thèse Doctorat, Ecole Centrale de Lyon, Lyon.

Crandall, S.H., Dahl, N.C. and Lardner, T.J. (1978), *An Introduction to the Mechanics of Solids*, McGraw-Hill, New York.

Fleck, N.A., Hutchinson, J.W. and Zhigang, S. (1991), "Crack path selection in a brittle adhesive layer", *Int. J. Solid. Struct.*, **27**(13), 1683-1703.

Follansbee, P.S. and Gray III, G.T. (1991), "Dynamic deformation of shock prestrained copper", *Mater. Sci. Eng. A*, **138**(1), 23-31.

Itoh, Y.Z., Suruga, S. and Kashiwaya, H. (1989), "Prediction of fatigue crack growth rate in welding residual stress field", *Eng. Frac. Mech.*, **33**(3), 397-407.

Juvé, D., Lourdin, P., Mbongo, B., Boukheit, N. and Treheux, D. (1993), "Damages and cracks in ceramic/metal interfaces", *J. Phys. IV*, **3**, 1057-1060.

Kang, K.J., Song, J.H. and Earmme, Y.Y. (1990), "Fatigue crack growth and closure behaviour through a compressive residual stress field", *Fatig. Fract. Eng. Mater. Struct.*, **13**(1), 1-13.

Kim, J.H. and Lee, S.B. (1998), "Stress intensity factors and crack initiation directions for ceramic/metal joint", *Theo. Appl. Fract. Mech.*, **30**(1), 27-38.

Kim, W.J., Lee, J.M., Kim, J.S. and Lee, C.J. (2012), "Measuring high speed Crack propagation In concrete fracture test using mechanoluminescent material", *Smart Struct. Syst.*, **10**(6), 547-555.

Kumar, S. and Barai, S.V. (2012), "Size-effect of fracture parameters for Crack propagation in concrete: a comparative study", *Comput. Concrete*, **9**(1), 1-19.

Liu, G. (2005), "Modélisation de l'essai d'indentation interfaciale en vue de caractériser l'adhérence de revêtements projetés thermiquement", Thèse Doctorat, Université des sciences et technologies de Lille, Lille.

Lourdin, P. (1992), "Les Liaisons Al2O3/Ni à l'état Solide, Elaboration: Etat des contraintes thermiques comportement mécanique", Thèse Doctorat, Ecole Centrale de Lyon, Lyon.

Mc Bain, J.W. and Hopkins, D.G. (1925), "On adhesives and adhesive action", *J. Phys. Chem.*, **29**(2), 188-204.

Mc Naney, J.M., Cannon, R.M. and Ritchie, R.O. (1994), "Near-interfacial crack trajectories in metal-

ceramic layered structures", *Int. J. Fract.*, **66**(3), 227-240.

Michel Dupeux (2004), Aide-mémoire de science des matériaux, IUT. 1er cycle/Licence, 2[éme] cycle/Master, Ecoles d'ingénieurs, Dunod, Paris.

Milan, M.T. and Bowen, P. (2000), "Fatigue crack growth resistance of selectively reinforced aluminum alloys", *Proceeding of the European Conference on Advances in Mechanical Behavior Plasticity and Damage*, Tours, France.

Milan, M.T. and Bowen, P. (2001), "Effects of particle size, volume fraction and matrix composition on the fatigue crack growth resistance on Al/Al+SiCp bi-materials", *Proceeding of the European Conference on Advances Materials and Process*, Rimini, Italy.

Product Dassault Systèmes Simulia Corp (2009), ABAQUS Standard Version 6.9, Providence, RI, USA.

Serier, B., Berroug, A., Juvé, D., Tréheux, D. and Moya, E. (1993), "Silver-alumina solid state bonding: Study of diffusion and toughness close to the interface", *J. Eur. Ceram. Soc.*, **12**(5), 385-390.

Shanahan, M.E.R. (1991), *Adhesion and wetting: Similarities and differences*, Rubber Word, October.

Shandhag, M.R., Eswaran, K. and Maiti, S.K. (1993), "Measurement of fracture toughness of bi-material interfaces and a stress based approach to their fracture", *Eng. Fract. Mech.*, **44**(1), 75-89.

Shih, C.F. and Asaro, R.J. (1988), "Elastic-Plastic Analysis of Cracks on Bi-material Interfaces: Part I-Small Scale Yielding", *J. Appl. Mech.*, **55**(2), 299-316.

Jiang, S.Y., Du, C.B. and Gu, C.S. (2014) "An investigation into the effects of voids, inclusions and minor Cracks on major Crack propagation by using XFEM", *Struct. Eng. Mech.*, **49**(5), 597-618.

Siddiq, M.A. (2006), "Modeling of crystal plasticity effects in the fracture of a metal/ceramic interface-bridging the length scales", Doctorate Thesis, Stuttgart University, Stuttgart.

Simmons, G. and Wang, H. (1971), *Single Crystal Elastic Constants and Calculated Aggregate Properties*, A Handbook, Second Edition, MIT Press, Cambridge, MA.

Touloukian, Y.S. (1967), "Thermophysical properties of high temperature solid materials", Purdue University, Thermo-physical Properties Research Center; Air Force Materials Laboratory (U.S.), MacMillan, New York.

Tvergaard, V. and Hutchinson, J.W. (1993), "The Influence of Plasticity on Mixed Mode Interface Toughness", *J. Mech. Phys. Sol.*, **41**, 1119-1135.